Performance analysis of water-to-water CO_2 heat pump in different compressor rotational speed

Yantong Li, *Natasa* Nord

Department of Energy and Process Engineering, Norwegian University of Science and Technology, Trondheim, Norway, yantong.li@ntnu.no

Abstract. Ozone layer depletion can be weakened when carbon dioxide (CO_2) replaces hydrochlorofluorocarbons and chlorofluorocarbons as the refrigerant in heat pumps. Performance investigations on water-to-water CO_2 heat pumps are still insufficient, especially in real life and experimental conditions. Seldom studies have reported that the compressor frequency may affect the performance of CO_2 heat pumps in some degree. However, the influence of compressor frequency on the performance of the water-to-water CO_2 heat pumps is still unknown. Hence, this study presented the experimental investigations on the water-to-water CO_2 heat pumps in different compressor frequency. The investigated CO_2 heat pump is located in the Energy and Indoor Environment Laboratory in the Department of Energy and Process Engineering at Norwegian University of Science and Technology. It is mainly composed of evaporator, compressor, gas cooler, liquid separator, internal heat exchanger, and expansion valve. The compressor was produced by the Officine Mario Dorin Spa. The plate heat exchangers were applied as evaporator, gas cooler, and internal heat exchanger. The PI controller controlled the discharge pressure by adjusting the expansion valve opening. Experimental cases in which the compressor rotational speed of 1,100 rev/min and 1,300 rev/min were conducted. The coefficient of performance (COP) was calculated by measuring the compressor power and heating capacity in the gas cooler. The analysis on the water-to-water CO_2 heat pump COP in different measured cases was depicted. This study therefore fills the research gap on the performance of the water-to-water CO_2 heat pump in different compressor rotational speed.

Keywords. Water-to-water, CO_2 heat pump, compressor rotational speed, experimental investigation.
DOI: https://doi.org/10.34641/clima.2022.53

1. Introduction

Huge energy needs that are caused by rapidly society development and population increasement, result in increasing the use of non-renewable energy including fossil fuels. This highly intensifies the environmental pollution [1]. Improvement of renewable energy use has become one of the primary tasks for humans. European Union has stated that by 2030 the portion of renewable energy in total energy use would be larger than 32% [2].

Heat pump obtaining thermal energy from ambient media, is one popular technique which enhances the renewable energy utilization. Scholars paid their attention on this aspect. Kosan and Aktas [3] concluded that the utilization of solar collector could enhance the performance of the system. Nikitin et al. [4] analyzed the performance of air-source and ground-source heat pumps in Saint Petersburg. It was found that the coefficient of performance (COP) of the air-source and ground-source heat pumps could reach up to 2.36 and 2.44, respectively. Boahen et al. [5] investigated the performance of the heat pump with different purposes including space heating and domestic hot water use. They found that the increase of returning hot water temperature led to the decrease of the system performance. Ural et al. [6] investigated a textile-based solar-assisted heat pump, and they found that the daily COP of this heat pump was higher than that of the conventional heat pump. Ahrens et al. [7] conducted the analysis of the energy system with the heat pump for both heating and cooling purposes. They concluded that the system COP could reach up to 4.1.

Compared with conventional heat pumps applying chlorofluorocarbons and hydrochlorofluorocarbons as refrigerants, heat pumps applying carbon dioxide (CO_2) as the refrigerant can cause less damage on the ozone layer. CO_2 heat pumps have become the research hotspot. Basso et al. [8] analyzed the performance of the CO_2 heat pump for solar cooling purpose, and they concluded that the COP of the CO_2 heat pump could reach up to 2.4. Humia et al. [9] conducted the study on a solar-assisted CO_2 heat pump, and they found that the maximum COP of the heat pump was approximately 3.67. Rony and Gladen [10] performed the investigation about a photovoltaic-assisted CO_2 heat pump. It was concluded that the COP of the system could reach up to 5.16. Rocha et al. [11] investigated a solar-assisted CO_2 heat pump. Their results indicated that the system COP was improved from 2.19 to 3.12 when solar irradiance increased from 6 W/m^2 to 969 W/m^2. Illán-Gómez et al. [12] studied the effect of different key variables on the performance of the CO_2 heat pump, and they concluded that outlet CO_2 temperature in gas cooler played a significant role on the system performance.

Seldom scholars began to focus on the studies on the effect of compressor rotational speed or frequency on the performance of the CO_2 heat pump, including the studies of Yang et al. [13] and Qin et al. [14]. Although in their studies the effect of compressor rotational speed or frequency on the CO_2 heat pump performance had been analyzed, the investigated CO_2 heat pump was air-source. More studies were urgently needed to verify the conclusions they have summarized. For example, the effect of different compressor rotational speed on the water-to-water CO_2 heat pump was still unknown.

This study therefore performed the experimental studies of the CO_2 heat pump in different compressor rotational speed, i.e., 1,000 rev/min and 1,300 rev/min. The experiments were conducted in the Energy and Indoor Environment Laboratory at the Department of Energy and Process Engineering, Norwegian University of Science and Technology. The PI controller was developed to fix the unchanged discharge pressure. For each compressor rotational speed, five cases with the discharge pressure varying from 7,300 kPa to 8,500 kPa with the interval of 300 kPa were conducted. The analysis on the heating capacity, power, COP, and expansion valve opening in these cases were presented.

The organization for remaining parts of this paper was depicted below. Section 2 presented the CO_2 heat pump experimental setup. The calculation of the uncertainties for measured COP was conducted in Section 3. Section 4 gave the results and detailed analysis for the measured cases. Important conclusions were summarized in Section 5.

2. CO_2 heat pump experimental setup

The CO_2 heat pump was in a laboratory of the Norwegian University of Science and Technology, and its schematic was depicted in Fig. 1. Table 1 depicts the information of important components in the investigated CO_2 heat pump. Note that the rated rotational speed, frequency, and displacement of the compressor were 1,450 rev/min, 50 Hz, and 4.06×10^{-4} m^3/s, respectively. The number of plates in the gas cooler, internal heat exchanger, and evaporator were 30, 12, and 40, respectively. The control of the fixed discharge pressure was conducted by the PI controller. Sensors from Carel having accuracy of ±(0.005×(measured temperature)+0.3) °C were applied for measuring temperature. A variable-area flow meter having accuracy of ±1% [15], was applied for measuring temperature. A sensor from Carel having accuracy of ±1% was applied for measuring pressure. A meter from CARLO GAVAZZI having accuracy of ±1% was applied for recording power.

Tab. 1 - Information of important components in CO_2 heat pump.

Components	Types	Manufactures
Compressor	CD 300H	Officine Mario Dorin Spa
Gas cooler	B18H-30	Swep International A.B.
Internal heat exchanger	CO42-12W-S3	KAORI Brazed Plate Heat Exchanger
Evaporator	CO95-40W-S37	KAORI Brazed Plate Heat Exchanger
Liquid separator	VU8L	Skala AS
Expansion valve	E2V18CS000	Carel

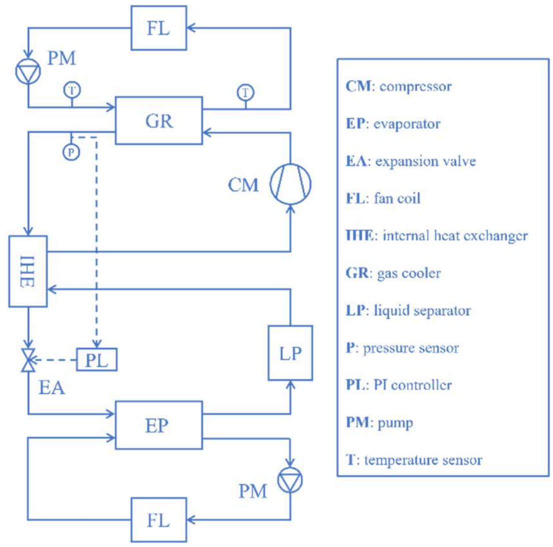

Fig. 1 – CO_2 heat pump experimental setup

3. Uncertainties for measured COP

This section was applied for presenting the calculation for uncertainties of measured variables. The CO_2 heat pump COP was calculated by Eqn. (1):

$$\mathrm{COP} = \frac{\dot{Q}_g}{P_c} \quad (1)$$

where $\dot{Q}_g$ and P_c denote the heating capacity and compressor power, respectively.

$\dot{Q}_g$ was calculated by Eqn. (2):

$$\dot{Q}_g = \dot{m}_g c_g (T_{gi} - T_{go}) \quad (2)$$

where $\dot{m}_g$ and c_g denote the mass flowrate and specific heat of the water in the gas cooler, respectively. T_{gi} and T_{go} denote the inlet and outlet water temperature of the gas cooler, respectively.

The root-sum-square method was applied for calculating uncertainties of measured variables, shown as Eqn. (3) [16]:

$$\varepsilon_v = \sqrt{\sum_{i=1}^{k} (\frac{\partial v}{\partial \beta_i} \varepsilon_{\beta_i})^2} \quad (3)$$

where v denotes the analyzed variable. β_i denotes the variable affecting v. ε_v and ε_{β_i} denote the uncertainties of v and β_i, respectively. This method was utilized for calculating uncertainties of measured variables in Eqns. (1) and (2). Uncertainty of COP ($\varepsilon_{\mathrm{COP}}$) was calculated by Eqn. (4):

$$\varepsilon_{\mathrm{COP}} = \sqrt{(\frac{\partial \mathrm{COP}}{\partial \dot{Q}_g} \varepsilon_{\dot{Q}_g})^2 + (\frac{\partial \mathrm{COP}}{\partial P_c} \varepsilon_{P_c})^2} \quad (4)$$

where $\varepsilon_{\dot{Q}_g}$ and ε_{P_c} denote the uncertainties of $\dot{Q}_g$ and P_c, respectively. $\varepsilon_{\dot{Q}_g}$ was calculated by Eqn. (5):

$$\varepsilon_{\dot{Q}_g} = \sqrt{(\frac{\partial \dot{Q}_g}{\partial \dot{m}_g} \varepsilon_{\dot{m}_g})^2 + (\frac{\partial \dot{Q}_g}{\partial T_{gi}} \varepsilon_{T_{gi}})^2 + (\frac{\partial \dot{Q}_g}{\partial T_{go}} \varepsilon_{T_{go}})^2} \quad (5)$$

where $\varepsilon_{\dot{m}_g}$, $\varepsilon_{T_{gi}}$, and $\varepsilon_{T_{go}}$ denote the uncertainties of $\dot{m}_g$, T_{gi}, and T_{go}, respectively. Using measured data, $\varepsilon_{\mathrm{COP}}$ could be determined by Eqns. (1) to (5). The average and maximum $\varepsilon_{\mathrm{COP}}$ were 3.7% and 4.27%, respectively.

4. Results and analysis

This section gave the results and analysis in different cases with the compressor rotation speed of 1,100 rev/min and 1,300 rev/min, respectively. The discharge pressure (P_d) was maintained at 7,300 kPa, 7,600 kPa, 7,900 kPa, 8,200 kPa, and 8,500 kPa, respectively. The heating capacity ($\dot{Q}_g$), compressor power (P_c), COP, and expansion valve opening (o_e) were selected as performance indicators.

4.1 Measured cases

Tables 1 and 2 presented the information of the measured cases with the compressor rotation speed of 1,100 rev/min and 1,300 rev/min, respectively. The water mass flowrate in gas cooler ($\dot{m}_g$) in these cases was 0.067 kg/s. In Table 1, the varying degree of the inlet water temperature in gas cooler (T_{gi}) in different P_d was small. The smallest T_{gi} was 25.4 °C, occurring when P_d was 7,301 kPa. The largest T_{gi} was 25.7 °C, occurring when P_d were 7,599 kPa and 8,200 kPa. The difference between smallest and largest T_{gi} was only 0.3 °C. The smallest T_{go} was 42 °C, occurring when P_d was 7,301 kPa. The largest T_{go} was 45.6 °C, occurring when P_d was 7,899 kPa. The difference between smallest and largest T_{go} was 3.6 °C. Thus, the difference of T_{go} was larger than that of T_{gi}.

In Table 2, the inlet water temperature in gas cooler (T_{gi}) increased from 25.2 °C to 27.1 °C, when P_d increased from 7,298 kPa to 8,503 kPa. The difference of T_{gi} between the cases with P_d of 7,298 kPa and 8,503 kPa was 1.9 °C. The outlet water temperature in gas cooler (T_{go}) increased from 44.5 °C to 51.5 °C, when P_d increased from 7,298 kPa to 8,503 kPa. The difference of T_{go} between the cases with P_d of 7,298 kPa and 8,503 kPa was 7 °C. The increasing degree of T_{go} was larger than that of T_{gi}, when P_d increased from 7,298 kPa to 8,503 kPa.

Tab. 1 – Measured cases with the compressor rotation speed of 1,100 rev/min.

Cases	P_d (kPa)	$\dot{m}_g$ (kg/s)	T_{gi} (°C)	T_{go} (°C)
1	7,301	0.067	25.4	42
2	7,599	0.067	25.7	43.6
3	7,899	0.067	25.6	45.6
4	8,200	0.067	25.7	45.1

5	8,356	0.067	25.5	45.4

Tab. 2 - Measured cases with the compressor rotation speed of 1,300 rev/min.

Cases	P_d (kPa)	$\dot{m}_g$ (kg/s)	T_{gi} (℃)	T_{go} (℃)
6	7,298	0.067	25.2	44.5
7	7,599	0.067	26.0	46.2
8	7,901	0.067	26.6	47.5
9	8,201	0.067	26.7	50.1
10	8,503	0.067	27.1	51.5

4.2 Effect on heating capacity

Fig. 2 presented the heating capacity ($\dot{Q}_g$) in different cases for different rotational speed: (a) $r =$ 1,100 rev/min and (b) $r =$ 1,300 rev/min. In Fig. 2 (a), when the compressor rotational speed was 1,100 rev/min, meaning that the compressor frequency was 37.9 Hz, $\dot{Q}_g$ was 4,626.3 W, 4,998.3 W, 5,603.7 W, 5,437.2 W, and 5,560.9 W in the Cases 1, 2, 3, 4, and 5, respectively. In Fig. 2 (b), when the compressor rotational speed was 1,300 rev/min, meaning that the compressor frequency was 55.8 Hz, $\dot{Q}_g$ was 5,396.2 W, 5,657.1 W, 5,857.4 W, 6,566.3 W, and 6,831.2 W in Cases 6, 7, 8, 9, and 10, respectively. Thus, when P_d was fixed at the almost same values, the increase of compressor frequency might lead to increase of $\dot{Q}_g$. This finding could be supported by the studies of Yang et al. [13] and Qin et al. [14]. In Fig. 2 (a), $\dot{Q}_g$ increased with the increase of P_d from Case 1 to Case 3. However, $\dot{Q}_g$ in both Cases 4 and 5 were lower than that in Case 3. The reason why $\dot{Q}_g$ in Case 4 and 5 were close might be that the unstable P_d control in Case 5 using PI controller. The setting P_d of 8,500 kPa cannot be maintained, even though the expansion valve opening has been adjusted to the minimum value, i.e., 10%. This is also the reason why P_d was 8,356 kPa in Table 1. In Fig. 2 (b), $\dot{Q}_g$ increased with the increase of P_d. The reason why the variations of $\dot{Q}_g$ was different in Figs. 2 (a) and (b) might be explained according to the study of Yang et al. [13]. In their study, P_d when the peak $\dot{Q}_g$ occurred increased with the increase of the compressor frequency.

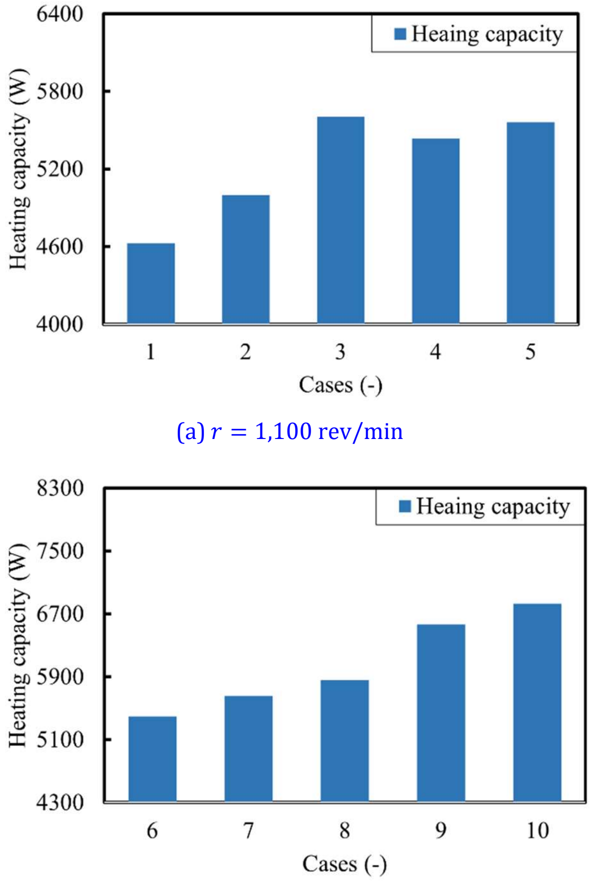

(a) $r =$ 1,100 rev/min

(b) $r =$ 1,300 rev/min

Fig. 2 – Heating capacity in different cases for different rotational speed: (a) $r =$ 1,100 rev/min and (b) $r =$ 1,300 rev/min.

4.3 Effect on compressor power

Fig. 3 presented the compressor power (P_c) in different cases for different rotational speed: (a) $r =$ 1,100 rev/min and (b) $r =$ 1,300 rev/min. In Fig. 3 (a), when the compressor rotational speed was 1,100 rev/min, meaning that the compressor frequency was 37.9 Hz, P_c was 1,066.1 W, 1,158.9 W, 1,235.8 W, 1,308 W, and 1,340.7 W in the Cases 1, 2, 3, 4, and 5, respectively. In Fig. 3 (b), when the compressor rotational speed was 1,300 rev/min, meaning that the compressor frequency was 55.8 Hz, P_c was 1,295.2 W, 1,381.7 W, 1,467.2 W, 1,540.4 W, and 1,610.4 W in the Cases 6, 7, 8, 9, and 10, respectively. Thus, when P_d was fixed at the almost same values, the increase of compressor frequency might lead to the increase of P_c. In addition, the increase of P_d might lead to the increase of P_c. These findings could be supported by the studies of Qin et al. [14].

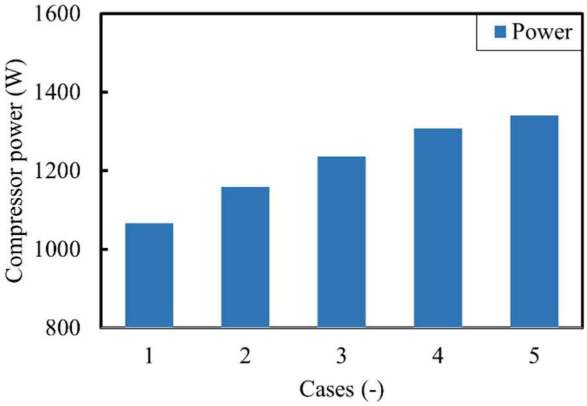

(a) r = 1,100 rev/min

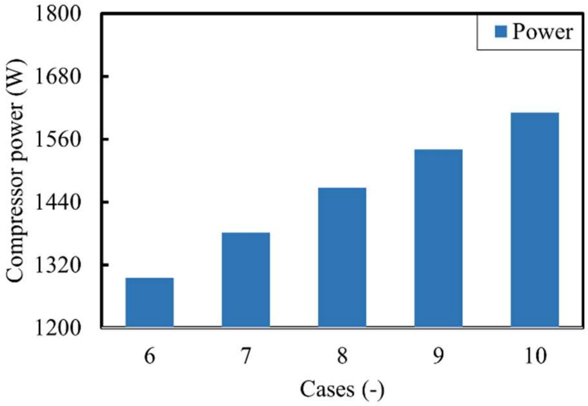

(b) r = 1,300 rev/min

Fig. 3 – Compressor power in different cases for different rotational speed: (a) $r = 1{,}100$ rev/min and (b) $r = 1{,}300$ rev/min.

4.4 Effect on COP

Fig. 4 presented the COP in different cases for different rotational speed: (a) $r = 1{,}100$ rev/min and (b) $r = 1{,}300$ rev/min. In Fig. 4 (a), when the compressor rotational speed was 1,100 rev/min, meaning that the compressor frequency was 37.9 Hz, COP was 4.34, 4.31, 4.53, 4.16, and 4.15 in the Cases 1, 2, 3, 4, and 5, respectively. In Fig. 4 (b), when the compressor rotational speed was 1,300 rev/min, meaning that the compressor frequency was 55.8 Hz, COP was 4.17, 4.09, 3.99, 4.26, and 4.26 in the Cases 6, 7, 8, 9, and 10, respectively. According to the study of Qin et al. [14], generally the decrease of the compressor frequency might lead to the increase of COP. In their study, there were still the phenomenon that in few cases the increase of compressor frequency might lead to the increase of COP. These could explain the phenomenon why COP in Cases 1, 2, and 3 were higher than that in Cases 6, 7, and 8, respectively, and why COP in Cases 4 and 5 were higher than that in Cases 9 and 10.

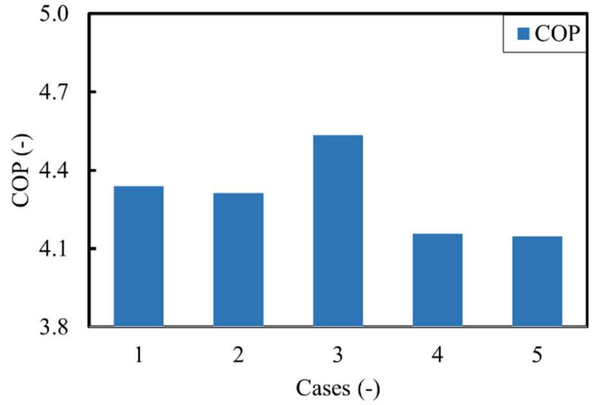

(a) r = 1,100 rev/min

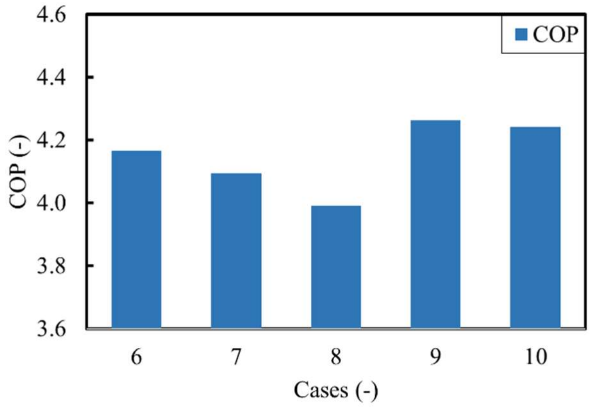

(b) r = 1,300 rev/min

Fig. 4 – COP in different cases for different rotational speed: (a) $r = 1{,}100$ rev/min and (b) $r = 1{,}300$ rev/min.

4.5 Effect on expansion valve opening

Fig. 5 presented the expansion valve opening (o_e) in different cases for different rotational speed: (a) $r = 1{,}100$ rev/min and (b) $r = 1{,}300$ rev/min. In Fig. 5 (a), when the compressor rotational speed was 1,100 rev/min, meaning that the compressor frequency was 37.9 Hz, o_e was 23.8%, 18.2%, 16.7%, 11.6%, and 10% in the Cases 1, 2, 3, 4, and 5, respectively. In Fig. 5 (b), when the compressor rotational speed was 1,300 rev/min, meaning that the compressor frequency was 55.8 Hz, o_e was 39.5%, 29.6%, 22.4%, 19.5%, and 18.1% in the Cases 6, 7, 8, 9, and 10, respectively. Thus, the increase of expansion valve opening might lead to the decrease of P_d. In addition, for maintaining at the almost same P_d, using higher compressor frequency might lead to larger expansion valve opening.

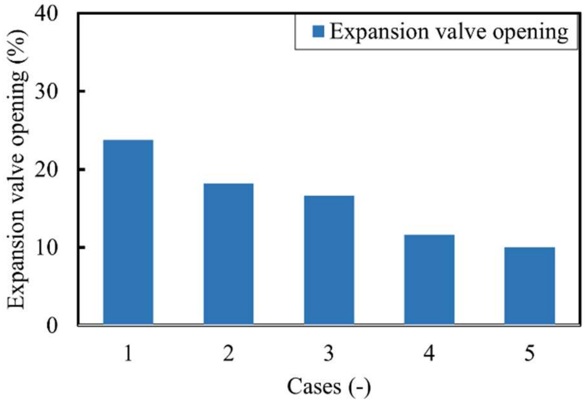

(a) $r = 1{,}100$ rev/min

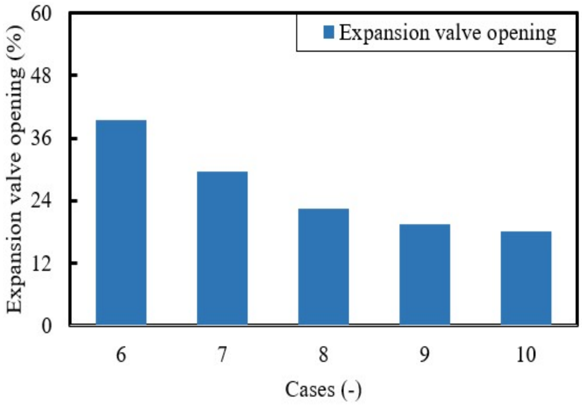

(b) $r = 1{,}300$ rev/min

Fig. 5 – Expansion valve opening in different cases for different rotational speed: (a) $r = 1{,}100$ rev/min and (b) $r = 1{,}300$ rev/min.

5. Conclusions

In this study, the performance of the CO_2 heat pump in different compressor rotational speed, i.e., 1,000 rev/min and 1,300 rev/min, were experimentally analyzed. The cases with the discharge pressure varying from 7,300 kPa to 8,500 kPa with the interval of 300 kPa were presented in experimental conditions. The heating capacity, power, COP, and expansion valve opening in these cases were analyzed. The uncertainties of the COP in these cases were calculated. The maximum and average uncertainties of the COP were 4.27% and 3.7%, respectively. Most findings of this study were compared with the results in the studies of Yang et al. [13] and Qin et al. [14]. Most findings on the effect of the compressor rotational speed on the performance of the CO_2 heat pump were verified. The results indicated that increasing the compressor rotational speed might result in increasing the heating capacity. Increasing the compressor rotational speed might result in increasing the compressor power. In most situations, reducing the compressor rotational speed might contribute to increasing the COP. However, there were still few cases where increasing the compressor rotational speed might contribute to increasing the COP. For maintaining at the almost same discharge pressure, the larger expansion valve opening might be caused by the higher compressor rotational speed. Note that these findings in this study were obtained by the unfixed operating conditions. As shown in Tables 1 and 2, the inlet water temperature of gas cooler in different cases were different. In addition, the measurement uncertainties might affect the results of these findings.

6. Acknowledgement

This project has received funding from the European Union's Horizon 2020 research and innovation programme under the Marie Skłodowska-Curie grant agreement No [895732].

7. References

[1] Ding Z., Wu W. A hybrid compression-assisted absorption thermal battery with high energy storage density/efficiency and low charging temperature. Applied Energy. 2021;282:116068.

[2] Commission E. 2030 climate & energy framework. 2021.

[3] Koşan M., Aktaş M. Experimental investigation of a novel thermal energy storage unit in the heat pump system. Journal of Cleaner Production. 2021;311:127607.

[4] Nikitin A., Deymi-Dashtebayaz M., Muraveinikov S, Nikitina V., Nazeri R., Farahnak M. Comparative study of air source and ground source heat pumps in 10 coldest Russian cities based on energy-exergy-economic-environmental analysis. Journal of Cleaner Production. 2021;321:128979.

[5] Boahen S., Anka SK., Lee KH., Choi JM. Performance characteristics of a cascade multi-functional heat pump in the winter season. Energy and Buildings. 2021;253:111511.

[6] Ural T., Karaca Dolgun G., Güler OV., Keçebaş A. Performance analysis of a textile based solar assisted air source heat pump with the energy and exergy methodology. Sustainable Energy Technologies and Assessments. 2021;47 :101534.

[7] Ahrens MU., Foslie SS., Moen OM., Bantle M., Eikevik TM. Integrated high temperature heat pumps and thermal storage tanks for combined heating and cooling in the industry. Applied Thermal Engineering. 2021;189:116731.

[8] Lo Basso G., de Santoli L., Paiolo R., Losi C. The potential role of trans-critical CO_2 heat pumps within a solar cooling system for building services: The hybridised system energy analysis

by a dynamic simulation model. Renew Energy. 2021;164:472-90.

[9] Marques Humia G., Moreira Duarte W., Jose Garcia Pabon J., de Freitas Paulino T., Machado L. Experimental study and simulation model of a direct expansion solar assisted heat pump to CO_2 for water heating: Inventory, coefficient of performance and total equivalent warming impact. Solar Energy. 2021;230:278-97.

[10] Rony RU., Gladen A.. Parametric study and sensitivity analysis of a PV/microchannel direct-expansion CO_2 heat pump. Solar Energy. 2021;218:282-95.

[11] Rocha TTM., de Paula CH., Maia AAT., Paulino TdF., de Oliveira RN. Experimental assessment of a CO_2 direct-expansion solar-assisted heat pump operating with capillary tubes and air-solar heat source. Solar Energy. 2021;218:413-24.

[12] Illán-Gómez F., Sena-Cuevas VF., García-Cascales JR, Velasco FJS. Analysis of the optimal gas cooler pressure of a CO_2 heat pump with gas bypass for hot water generation. Applied Thermal Engineering. 2021;182:116110.

[13] Yang L-X., Wei X-L., Zhao L-H., Qin X., Zhang D-W. Experimental study on the effect of compressor frequency on the performance of transcritical CO_2 heat pump system with regenerator. Applied Thermal Engineering. 2019;150:1216-23.

[14] Qin X., Liu H., Meng X., Wei X., Zhao L., Yang L. A study on the compressor frequency and optimal discharge pressure of the transcritical CO_2 heat pump system. International Journal of Refrigeration. 2019;99:101-13.

[15] ToolBox TE. Accuracy of variable-area flowmeter. 2021.

[16] Moffat RJ. Describing the uncertainties in experimental results. Experimental thermal and fluid science. 1988;1:3-17.